Structure, Vol. 11, 1595–1607, December, 2003, ©2003 Elsevier Science Ltd. All rights reserved. DOI 10.1016/j.str.2003.11.002

Protein Kinase A in Complex with Rho-Kinase Inhibitors Y-27632, Fasudil, and H-1152P: Structural Basis of Selectivity

Christine Breitenlechner,[1] Michael Gaßel,[2] Hiroyoshi Hidaka,[4] Volker Kinzel,[2] Robert Huber,[1] Richard A. Engh,[1,3,*] and Dirk Bossemeyer[2,*]

[1]Abteilung Strukturforschung
Max-Planck-Institut fuer Biochemie
82152 Martinsried

[2]Department for Pathochemistry
German Cancer Research Center
69120 Heidelberg

[3]Department of Medicinal Chemistry
Roche Diagnostics GmbH
82372 Penzberg
Germany

[4]D-Western Therapeutics Institute
Yagota Building 2C
100-32 Yagotohonmachi
Showa-ku, Nagoya 466 0825
Japan

Summary

Protein kinases require strict inactivation to prevent spurious cellular signaling; overactivity can cause cancer or other diseases and necessitates selective inhibition for therapy. Rho-kinase is involved in such processes as tumor invasion, cell adhesion, smooth muscle contraction, and formation of focal adhesion fibers, as revealed using inhibitor Y-27632. Another Rho-kinase inhibitor, HA-1077 or Fasudil, is currently used in the treatment of cerebral vasospasm; the related nanomolar inhibitor H-1152P improves on its selectivity and potency. We have determined the crystal structures of HA-1077, H-1152P, and Y-27632 in complexes with protein kinase A (PKA) as a surrogate kinase to analyze Rho-kinase inhibitor binding properties. Features conserved between PKA and Rho-kinase are involved in the key binding interactions, while a combination of residues at the ATP binding pocket that are unique to Rho-kinase may explain the inhibitors' Rho-kinase selectivity. Further, a second H-1152P binding site potentially points toward PKA regulatory domain interaction modulators.

Introduction

Protein kinases are phosphorylation enzymes that control cellular signaling events and accordingly may cause a wide range of diseases when defective. Since they are typically active only when signaling, most of the diseases associated with protein kinase deregulation (including the majority of all cancers) arise from excess activity due to mutation, overexpression, or disabled cellular inhibition. Other protein kinases contribute to disease in the course of their normal function in cellular processes such as cell survival or cell migration. The prevalence of kinases to cause or augment disease underscores the need for therapeutic protein kinase inhibitors, with the caveat that they must be highly selective for their disregulated targets to avoid inhibition of other ubiquitous but essential protein kinases. Several protein kinase inhibitors have been approved for human treatment or are in advanced clinical trials. The first was fasudil (HA-1077 or AT877), which was approved in 1995 for the treatment of cerebral vasospasm, a painful and potentially deadly result of subarachnoid hemorrhage. Fasudil has significant vasodilatatory activity (Ono-Saito et al., 1999) and is now undergoing clinical trials for the treatment of angina pectoris (Shimokawa et al., 2001). Fasudil's activity has been attributed to inhibition of Rho-kinase (Matsui et al., 1996) and its role in signaling for myosin light chain phosphorylation and arterial smooth muscle contraction (Amano et al., 1996), although the in vitro activity of fasudil is not strictly limited to Rho-kinase. Other Rho-kinase-related protein kinases, such as PKA, PRK2, MSK1, and S6K1, are also inhibited by fasudil, although to a lesser extent (Davies et al., 2000). Fasudil is related to H7, an isoquinoline sulfonamide derivative that is a weak PKC inhibitor (Hidaka et al., 1984) and whose protein kinase binding mode was shown by the cocrystal structure with PKA (Engh et al., 1996). Fasudil has a heptameric homopiperazine ring at the position of the methyl-piperazine ring of H7 (Figure 1). Further derivitization of fasudil led to H-1152P, with two additional methyl groups, one at the isoquinoline ring and the other at the homopiperazine ring (Tanaka et al., 1998). H-1152P has a better inhibitory profile than HA-1077, with a K_D value for Rho-kinase in the low nanomolar range and a reportedly enhanced selectivity (Tanaka et al., 1998; Sasaki et al., 2002). Rho-kinase may be an important pharmacological target also for cancer because of its role in the phosphorylation of focal adhesion kinase (Sinnett-Smith et al., 2001) and the invasion and migration of cancer cells (for reviews, see Fukata et al., 2001; Amano et al., 2000). Regarding the latter, Itoh et al. (1999) showed that the migration of rat MM1 hepatoma cells was prevented by the Rho-kinase inhibitor Y-27632. As a pyridine derivative, Y-27632 differs in its chemical structure from H inhibitors described above. It has a K_D of 140 nM for Rho-kinase and 25 μM for PKA (Ishizaki et al., 2000) and is ATP competitive, like the H inhibitors (Trauger et al., 2002; Ikenoya et al., 2002).

Crystal structure analyses of protein kinase inhibitor complexes reveal the intermolecular interactions responsible for ligand binding and thereby enable structure-based rational design and optimization of kinase inhibitors. To date, crystal structures have been determined for some 30 protein kinases, representing less than 6% of the 518 protein kinases in the human genome (Manning et al., 2002). Many of these structures have been complexes with protein kinase inhibitors, but most have shown an inactive state. As a serine-threonine kinase of the AGC group, Rho-kinase possesses a cata-

*Correspondence: d.bossemeyer@dkfz.de (D.B.), engh@biochem.mpg.de (R.A.E.)

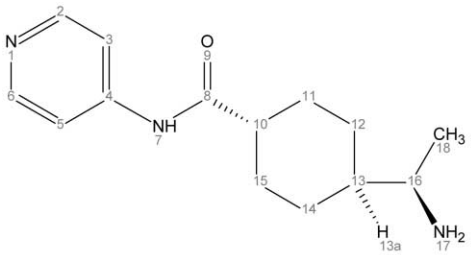

Y-27632

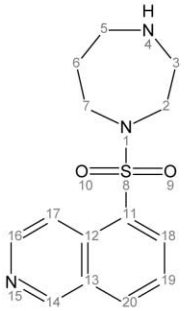

HA-1077

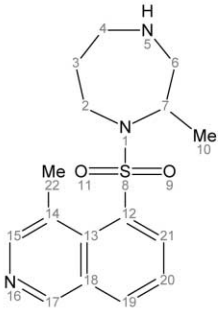

H-1152P

Figure 1. Chemical Structures of the Inhibitors Y-27632, HA-1077, and H-1152P

lytic domain closely related to other AGC group kinases, among them PKA, PKB, PKC, and PKG, although no crystal structure of Rho-kinase has been reported. The close relationship between PKA and Rho-kinase and the well established crystallization conditions for PKA make PKA a suitable model system for studying Rho-kinase inhibitors. Furthermore, cocrystallization of PKA with Rho-kinase inhibitors helps identify factors governing cross selectivity of protein kinase inhibitors, a major concern in protein kinase inhibitor design.

The ATP binding site residues conserved between PKA and Rho-kinase include Phe327 (PKA numbering). This residue is a characteristic but not absolutely conserved feature of the AGC group of kinases. It is positioned on the C-terminal polypeptide strand which stretches between the α helical catalytic domain lobe and the C-terminal anchor in the hydrophobic motif. Phe327 shields one side of the ATP pocket and lies adjacent to the adenine of ATP and aromatic groups of ATP-site inhibitors (Prade et al., 1997; Engh et al., 1996). Rho-kinase and PKA differ, however, in eight positions in the ATP binding pocket (Figure 2). Four of their side chains are in close ($<$4 Å) contact with the inhibitors, corresponding to the following PKA→Rho substitutions: Leu49Ile, Val123Met, Thr183Ala, and Glu127Asp. Because the protein kinase fold is so highly conserved, variations of amino acid residues that line the ATP subsite belong to the most important factors in defining inhibitor selectivity. Here we describe the crystal structures of PKA in complex with HA-1077 (at 2.2 Å resolution), with H-1152P (1.9 Å), and with Y-27632 (2.0 Å) and analyze the factors governing their relative affinities for PKA and Rho-kinase. The structures identify the binding interactions of the inhibitors in the ATP pocket. The surface areas of the inhibitor/PKA interface correlate well with their inhibitory activities. Furthermore, the specific sequence differences between PKA and Rho-kinase provide an explanation for the observed higher affinity of these molecules for Rho-kinase. On the basis of these structural data, we propose models for the Rho-kinase-specific binding modes that rationalize the roles of the unique combination of amino acid residues found in the Rho-kinase ATP binding pocket. In addition, a second, well ordered H-1152P molecule was observed in a surface region with contact to the phosphoryl group of Thr197 and to Lys189, both from the activation loop, and to Glu86 from Helix C, a region critical for kinase activity and protein-protein interaction.

Results and Discussion

Overall Structure

The PKA complexes with Rho-kinase inhibitors Y-27632 (PKA-Y), fasudil or HA-1077 (PKA-1077), and H-1152P (PKA-1152) were cocrystallized as ternary complexes with the recombinant catalytic subunit of cyclic AMP-dependent protein kinase (PKA) and the pseudo-substrate kinase inhibitor peptide [PKI(5-24)]. All three inhibitor complexes crystallized in the orthorhombic space group $P2_12_12_1$. The PKA-1152 and PKA-Y crystals have similar cell constants (ca. 74.1, 76.6, 81.0) and the same crystal packing arrangement (Table 1). PKA-1077 has slightly different cell constants (70.33, 73.67, 79.08) and different crystal contacts. The inhibitor molecules occupy the ATP binding site; H-1152P binds additionally at a second site bounded by pThr197, helix C residues, and residues from the PKI(5-24) peptide of a symmetry related molecule. Apart from that, no direct contacts exist between any of the inhibitors and PKI(5-24).

Open and Closed Conformations

Ligand-induced conformational changes have been well documented for PKA (Prade et al., 1997; Johnson et al., 2001). Foremost among these are variations in the relative orientations of N- and C-terminal lobes, whose interface creates the ATP binding pocket. The "openness" of the pocket ranges from "closed" for PKA structures with bound ATP or AMPPNP (PDB code 1ATP, 1CDK) in the presence of pseudosubstrate, "closed" or "intermediate" for various inhibitors, to "open" for unliganded PKA (PDB code 1J3H; Akamine et al., 2003). The extent of openness can be quantitatively characterized by using several parameters. One is the occurrence of a hydrogen bonding distance between NE2 of His87 from helix C and pThr197 (O3P) of the activation loop in the closed conformation. By this measure, the structures of PKA-Y and PKA-1152 (Figure 3, green ribbon, 2.5 Å; yellow ribbon, 2.6 Å) represent closed lobe structures, whereas the PKA-1077 structure is—with a 4.6 Å separation—an open structure (Figure 3, red ribbon).

Glycine Loop

The flexibility of the glycine loop is demonstrated by relatively high B factors and by the occurrence of dif-

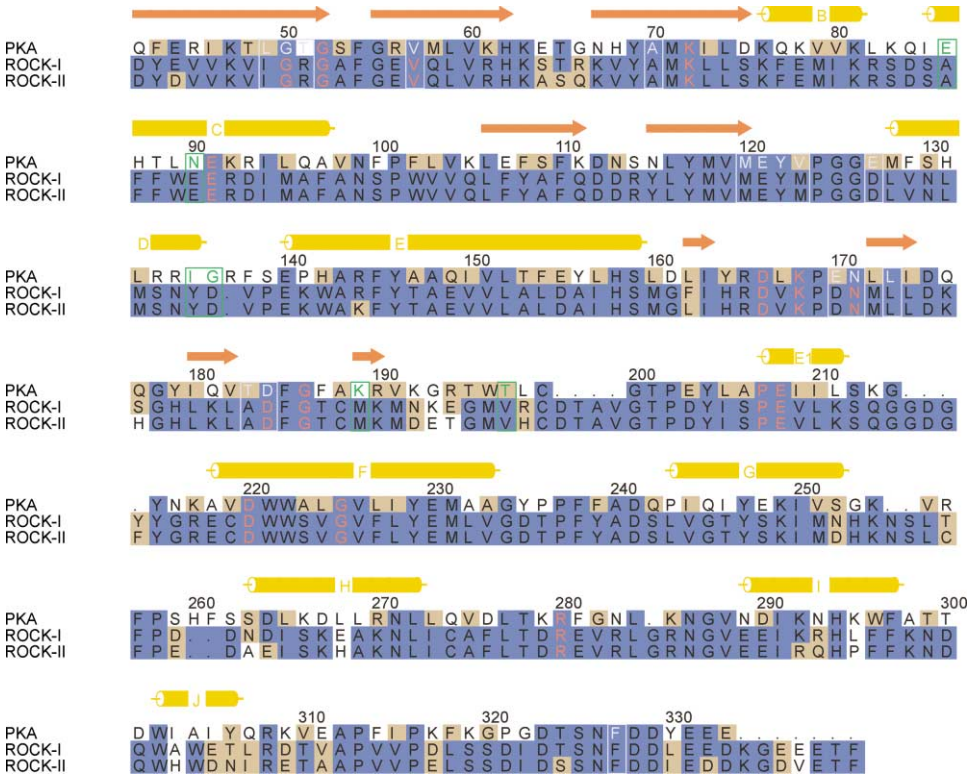

Figure 2. Sequence Alignment of PKA and the Highly Similar Rho Kinase Family Members ROCK-I and ROCK-II

Blue backgrounds indicate identical residues whereas brown indicates conservative exchanges. Secondary structure elements of PKA (from Bossemeyer et al., 1993) are indicated above the PKA numbering. The most highly conserved kinase residues are shown in red letters. Inhibitor contacts are marked with light violet letters and boxes. Additionally, contacts with H-1152P in the second binding site are indicated in green.

ferent positions in all three structures. The differing positions create ATP ligand binding sites that are progressively more open among structures 1CDK (PKA/PKI(5-24)/MnAMP-PNP) (Bossemeyer et al., 1993), PKA-Y, PKA-1152, and PKA-1077 (3, 4) (Figure 3C, blue, green, yellow, and red ribbon, respectively). There is also evi-

Table 1. Data Collection and Refinement Statistics

	Y-27632	H-1152P	HA-1077
Data Collection			
Space group	$P2_12_12_1$	$P2_12_12_1$	$P2_12_12_1$
Cell (a, b, c) (Å)	74.0, 76.6, 80.7	74.2, 76.4, 81.8	70.3, 73.7, 79.1
Resolution range (Å)	15.8–2.0	10.91–1.9	20–2.2
Completeness (%) [last shell]	97.8 [88.7]	91.8 [56.0]	82.4 [59]
$I/\sigma(I)$ [last shell]	4.2 [1.4]	7.5 [0.6]	7.5 [1.3]
R_{sym} [last shell]	0.12 [0.50]	0.06 [0.51]	0.10 [0.34]
Refinement			
Number of atoms used in refinement	3104	3245	2914
R factor (%)	18.1	17.9	21.7
Free R factor (%)	22.9	21.7	29.3
Free R value test size (%)	10.1	5.0	5.0
Reflections used	27,774	32,327	16,761
Standard Deviation from Ideal Values			
Bond length (Å)	0.016	0.017	0.021
Bond angles (°)	1.440	1.491	1.83
Temperature Factors			
All atoms	39.4	25.1	24.4
Main chain/side chain atoms PKA	37.6/40.0	22.9/25.5	23.1/25.2
Main chain/side chain atoms PKI	32.8/36.7	21.0/23.9	26.6/29.8
Inhibitor atoms	38.3	33.3	23.2
Solvent molecules	50.3	36.6	25.8
Inhibitor atoms (second)		21.2	
Detergent		43.3	

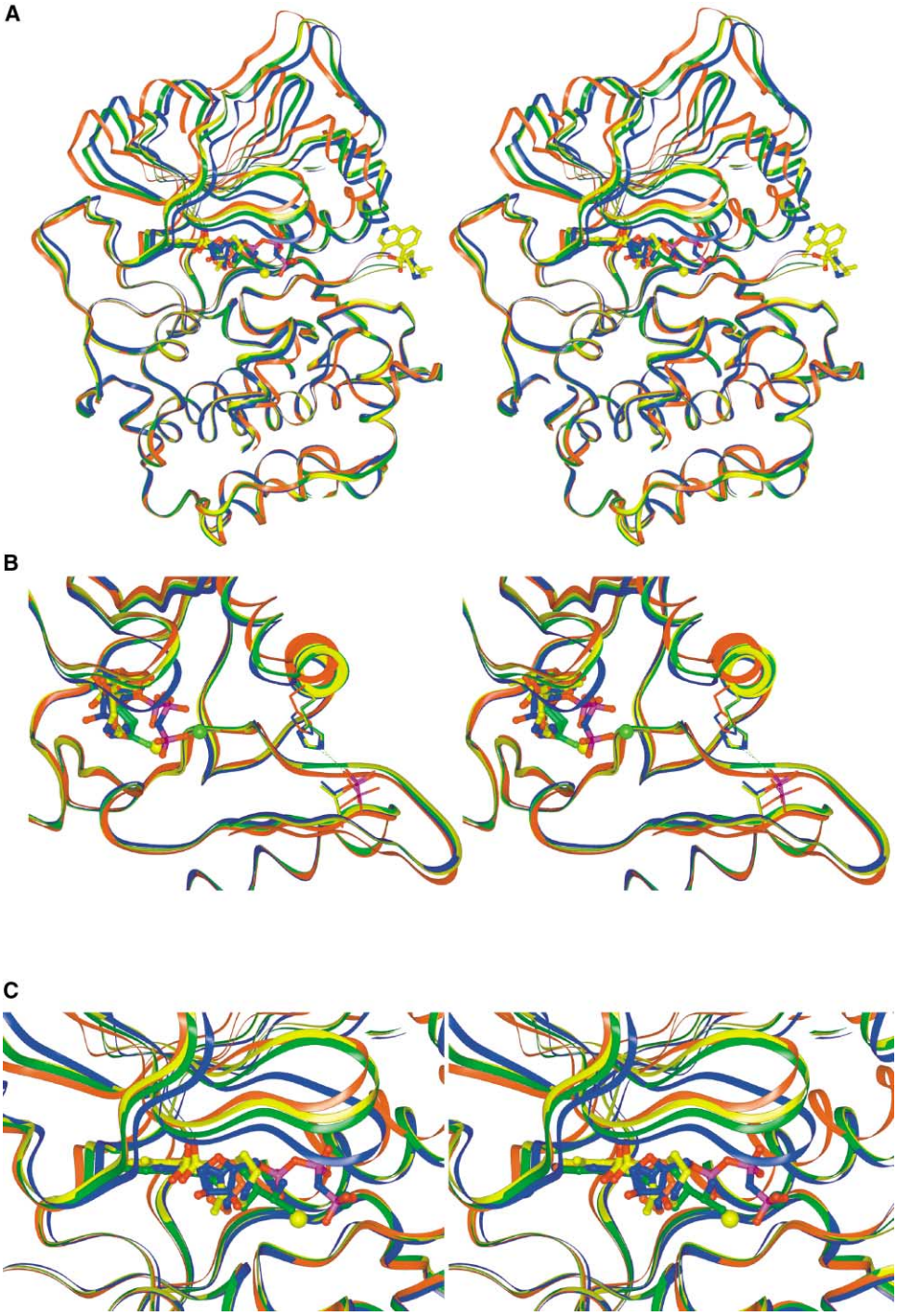

Figure 3. Binding of the Inhibitors to PKA

(A) Open-closed conformations illustrated by an overlay of all three inhibitor structures (Y-27632, green; HA-1077, red; H-1152P, yellow) and the PKA-AMP-PNP (1CDK) complex (blue) for comparison.

(B) In the PKA-HA1077 structure, helix C is further away from the activation loop, and the salt bridge His87-pThr197 is not formed.

(C) A closer view of the binding pocket shows the inhibitor binding modes relative to AMP-PNP and the positions of the flexible glycine-loop. The inhibitor molecules occupy both the adenine and the ribose pocket, but not the triphosphate binding site.

dence for multiple conformations of the glycine flap within a single crystal (data not shown). PKA-Y electron density maps suggest the partial occupancy of a more closed position of the glycine flap (especially involving turn residues Ser53-Phe54-Gly55), similar to that previously observed with the H7 and H8 inhibitor complex structures of PKA (Engh et al., 1996). Because none of the cocrystallized inhibitors occupies this site, they do

not have the structuring effect of the triphosphoryl group of ATP with its contacts to the glycine loop.

Inhibitor Binding

The chemical structures of the three inhibitors are shown in Figure 1. They originate from two different chemical classes but share the general architecture of a planar ring system linked to a saturated ring. In the case of Y-27632, a pyridine ring is connected by an amide to a saturated para-aminoethyl cyclohexane ring. HA-1077 and its derivative H-1152P share the basic scaffold of an isoquinoline ring connected to a homopiperazine ring by a sulfonamide linker. Compared to HA-1077, H-1152P has two additional methyl groups, one at the isoquinoline ring and another at the homopiperazine ring. These two methyl groups are thus responsible for the unique binding properties of the derivative. The planar ring systems occupy the adenine subsite, while the linker and the saturated rings occupy the ribosyl subsite. The triphosphate subsite is not used by any of the inhibitors (Figures 3C and 4).

Figure 4 shows the inhibitors in the ATP pocket and the F_o-F_c electron density maps with the inhibitor atoms omitted contoured at 2.5σ. Y-27632 is well defined in the electron density (Figure 4A), which, however, does not uniquely identify the orientation of the cyclohexane ring chair conformer (see next paragraph). The typical intrinsic flexibility of the seven-membered homopiperazine rings of HA-1077 and H-1152P is reflected in less well defined electron densities in this region (Figures 4B and 4C). The electron density of H-1152P (Figure 4C) has gaps in portions of the homopiperazine ring too, contradicting expectations that the two extra methyl groups should stabilize the ring conformations relative to HA-1077. In contrast, the homopiperazine ring of the H-1152P inhibitor bound outside the catalytic cleft close to Thr197 of the activation loop binds with a clearly defined electron density for the whole inhibitor (Figure 4D).

Binding of Y-27632

With a K_D value of 17.5 $\pm$ 3.87 μM by surface plasmon resonance spectroscopy (SPR) and a 25 μM K_i value from previous kinetic data (Uehata et al., 1997), Y-27632 has the weakest PKA inhibition of the compounds studied here (Table 2). For Rho-kinase, however, Y-27632 has a K_i value of 140 nM. This pronounced selectivity for Rho-kinase is further emphasized by data showing that Y-27632 inhibited only one other protein kinase (PRK2) from a panel of 34 kinases with similar potency (Davies et al., 2000).

Despite the relatively weak PKA inhibition, Y-27632 cocrystallized readily and is clearly localized in the electron density, although two orientations of a chair conformer of the cyclohexane ring are possible (Figure 4A). To analyze the binding of Y-27632 to PKA, we considered binding surfaces and hydrophobic (van der Waals), and hydrophilic (H bonds) interactions for both conformations (see Tables 3–5). The buried surface areas (188 or 189 Å^2) and numbers of van der Waals contacts (64 or 67) are similar for the two conformations. The van der Waals contacts are formed to residues from the ATP binding pocket, especially to the invariable Val57 with 9 or 10 side chain contacts and to the more variable Val123 with 12 contacts. Four contacts are formed to Phe327, the residue characteristic of the AGC kinases that is inserted into the ATP pocket from the C-terminal strand of the kinase. The two conformations differ most at the terminal aminoethyl group, which adopts either one H bond between N17 and the backbone carbonyl oxygen of Thr51 (2.83 Å) (Table 4; Figure 5A), or a H bond with Asn171 (OD1) (2.89 Å) and Asp184 (OD1) (2.93 Å) (Table 4). The pyridine ring in both conformations forms a H bond between pyridine nitrogen atom N1 and backbone nitrogen of Val123 (2.93 Å) (Figure 5A), the hydrogen bond donor at the hinge region between the N- and C lobes that binds to nearly all known ATP-site inhibitors (Engh and Bossemeyer, 2001). Y-27632 also binds via water molecules sandwiched between N7 and the carboxylate of Glu127 and the backbone carbonyl of Leu49.

HA-1077

As described in the introduction, HA-1077, also known as fasudil, is used to treat cerebral vasospasm and works via Rho-kinase inhibition. However, it also inhibits several other kinases in the μM range (Davies et al., 2000). Our SPR data show a K_D value of 5.7 μM for PKA; published data include a K_i value of 1.0 μM (Ikenoya et al., 2002) (Table 2). HA-1077 makes three H bonds to PKA (Figure 5B; Table 4). Like other isoquinoline inhibitors (Engh et al., 1996), one H bond is formed between the isoquinoline N (N15) to the backbone N of Val123 (2.8 Å). The homopiperazine amine (N4) forms H bonds with the backbone carbonyl oxygen of Glu170 (3.25 Å) and the side chain of Glu127 (OE2) (2.69 Å), the latter at the position of the ribose 3′OH group in the ATP-PKA complex (Bossemeyer et al., 1993). A Glu127-inhibitor contact was observed for staurosporine (Prade et al., 1997), but not with the other isoquinoline sulfonamide inhibitors (Engh et al., 1996). A total of 81 van der Waals contacts are formed to the residues of the ATP pocket. Most contacts are to Val123 (13), Val57 (11), and Thr183 (11) (Table 4).

H-1152P

H-1152P is a derivative of HA-1077 with enhanced specificity for Rho-kinase (Sasaki et al., 2002). For PKA, it has a K_D (SPR) or K_i (Ikenoya et al., 2002) value of 1.06 or 0.63 μM, respectively (Table 2). With a K_i of 1.6 nM, H-1152P inhibits Rho-kinase potently (Sasaki et al., 2002; Ikenoya et al., 2002). The H-1152P molecule that binds to the ATP pocket makes only one H bond contact (from the isoquinoline N [N16] to the backbone NH of Val123 [3.0 Å]) (Figure 5C; Table 3). As with the other inhibitors described here, Val57 and Val123 are involved in many van der Waals contacts; in contrast to the other two inhibitors, Leu173 and Leu49 additionally form many contacts (Leu173: 12 with H-1152P versus 2 with HA-1077; and Leu49: 8 with H-1152P versus 2 with Y-27632 and 4 with HA-1077).

In its second binding site close to helix C and the activation segment, H-1152P makes five H bond contacts, three to the Thr197-phosphoryl group in the acti-

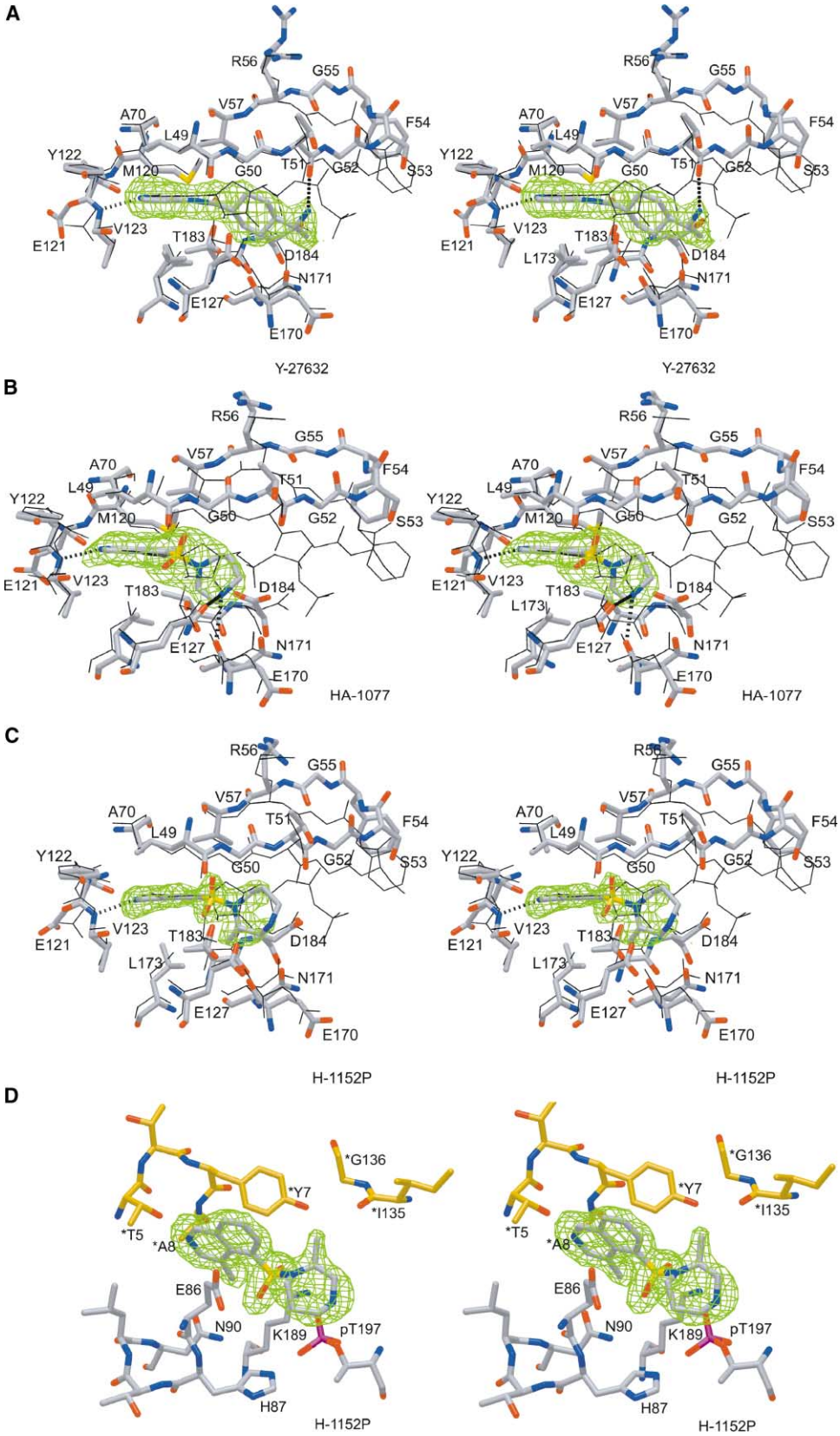

Figure 4. Structure of Inhibitor Binding Sites with Electron Density Maps

Shown are the three PKA bound inhibitors with corresponding F_o-F_c electron density maps (inhibitor atoms omitted) contoured at 2.5σ. Amino acid residues in the vicinity of the inhibitors are shown. H bonds between inhibitor atoms and enzyme residues are depicted as dotted lines. The PKA-PKI-AMP-PNP complex is drawn as fine black lines. Inhibitors (A) Y-27632, (B) HA-1077, and (C) H-1152P bind in the ATP pocket. (D) The second H-1152P molecule, which occupies a binding site at the enzyme surface in contact with the activation loop and helix C, is well ordered, indicated by its well defined electron density. (Residues from a symmetry-related molecule are colored yellow.)

Table 2. Inhibitor Binding Properties

Inhibitor	Y-27632	HA-1077	H-1152P
K_D PKA	17.5 ± 3.9 μM	5.7 ± 1.2 μM	1.1 ± 0.1 μM
K_i PKA[a]	25 μM	1.0 μM	0.63 μM
K_i RHO[a]	0.14 μM	0.33 μM	0.0016 μM
Buried surface	188(189)	196.4	215.7
VDW contacts	64(67)	81	96
H bonds	2(3)	3	1

K_D values from surface plasmon resonance spectroscopy (SPR) analysis, Chi^2 smaller than five, two independent experiments, Inhibition constants correlate well with the buried surface and number of van der Waals (VDW) contacts but not with number of H bonds.
[a] K_i values from literature (Ikenoya et al., 2002; Sasaki et al., 2002).

vation loop, one to Lys189 also of the activation loop, and one to Thr5 of PKI(5-24) from a symmetry-related molecule (Figure 5D). The inhibitor is embedded in a network of water molecules, thus making additional contacts via water to Asn90 from helix C and Thr195 from the activation loop. In this activation loop binding site, the inhibitor electron density is well connected and verifies a unique conformation of the homopiperazine ring with no apparent disorder (Figure 4D). Significant van der Waals contacts are made to the side chain of Glu86 from helix C, which changes its side chain conformation (compared to 1CDK) to accommodate the inhibitor. Further binding studies are necessary to determine the relevance of the second binding site in solution.

Binding Specificities of Y-27632, HA-1077, and H-1152P

Comparison with the Mn^{2+}-AMP-PNP complex identifies only small induced-fit movements of ATP pocket residues associated with binding of the three inhibitors. The side chain of Asp184, which chelates a metal ion in the active complex, is oriented toward the opening of the active side cleft in the AMP-PNP complex and in the PKA-Y or PKA-1152 structure. In the PKA-1077 structure, however, Asp184 adopts a different rotamer (Figure 5B), which points toward the homopiperazine ring, increasing van der Waals contacts and apparently enhancing hydrophobic effect binding. A similar reorientation of this side chain was observed in the H8-inhibitor complex of PKA (Engh et al., 1996), where Asp184 makes an H bond contact to the amide of the inhibitor side chain. Thr183 and Leu173 in the PKA-Y structure apparently have two conformations that were each modeled with an occupancy of 0.50 (data not shown). These two amino acid residues interact with each other by van der Waals contacts which limit their degree of conformational freedom, indicating mutually dependent rotamer conformations and a concerted induced fit movement.

The three inhibitors bind with moderate binding strengths to PKA. Their differing affinities (Table 2) correlate with the different numbers of van der Waals contacts and with the contact surface area between the inhibitors and enzyme residues (buried surface) (Table 2). H-1152P, which has the highest affinity for PKA, also has the highest number of van der Waals contacts and the largest buried surface (215.7 $Å^2$). Y-27632, with the weakest PKA binding, has the smallest total number of van der Waals contacts and a buried surface area of 189.9 $Å^2$. A relationship of buried surface areas and affinities of PKA inhibitors has been noted previously (Engh and Bossemeyer, 2002). The simplest measure of hydrophilic binding interactions—the number of inhibitor-protein H bonds—does not correlate with PKA binding affinities. This is typical of enzyme inhibitors and reflects the existence of competing hydrophilic interactions in inhibitor solvation. H-1152P possesses only a single H bond from its isoquinoline ring to Val123 in the hinge region. This H bond to Val123 or its equivalent is nearly universal among protein kinase-inhibitor complexes and exists in all PKA-inhibitor complexes crystallized so far (Narayana et al., 1999; Prade et al., 1997; Engh et al., 1996). Indeed, a survey of ligand binding properties from protein kinase crystal structures in the protein data bank identifies only two inhibitors that lack such an interaction, namely CK2/Emodin (1F0Q) (Battistutta et al., 2000) and p38/BPU (1KV1). All other ligands make one, two, or three H bonds to the hinge polypeptide, i.e., always one to the hinge region backbone amide of the Val123

Table 3. Van der Waals Contacts of the Inhibitors to PKA Enzyme Residues

Residue	Y Chair1	Y Chair2	HA-1077	H-1152P	Interaction via
L49	2	2	4(1p*)	8(1p*)	main chain/side chain
G50	—	1	2	4(1p*)	main chain
T51	3	3	—	5	main chain
V57	9	10	11	12	side chain
A70	4	4	6	7	side chain
M120	1	1	4	4	side chain
E121	2(1p*)	2(1p*)	3(1p*)	3(1p*)	main chain
Y122	6	6	7	6	main chain/side chain
V123	12	12	13	10(1p*)	main chain/side chain
E127	—	—	4	4(2p*)	side chain
E170	2	2	2	4	main chain
N171	6	4	2	2	main chain/side chain
L173	5	6	2	12	side chain
T183	4(1p*)	6(1p*)	11	7	side chain
D184	4	4	4	—	side chain
F327	4	4	6	8	side chain
Total	64(2p*)	67(2p*)	81(2p*)	96(6p*)	

Residues that have side chain contacts with the ATP-site ligands and differ between Rho-kinase and PKA are in bold.

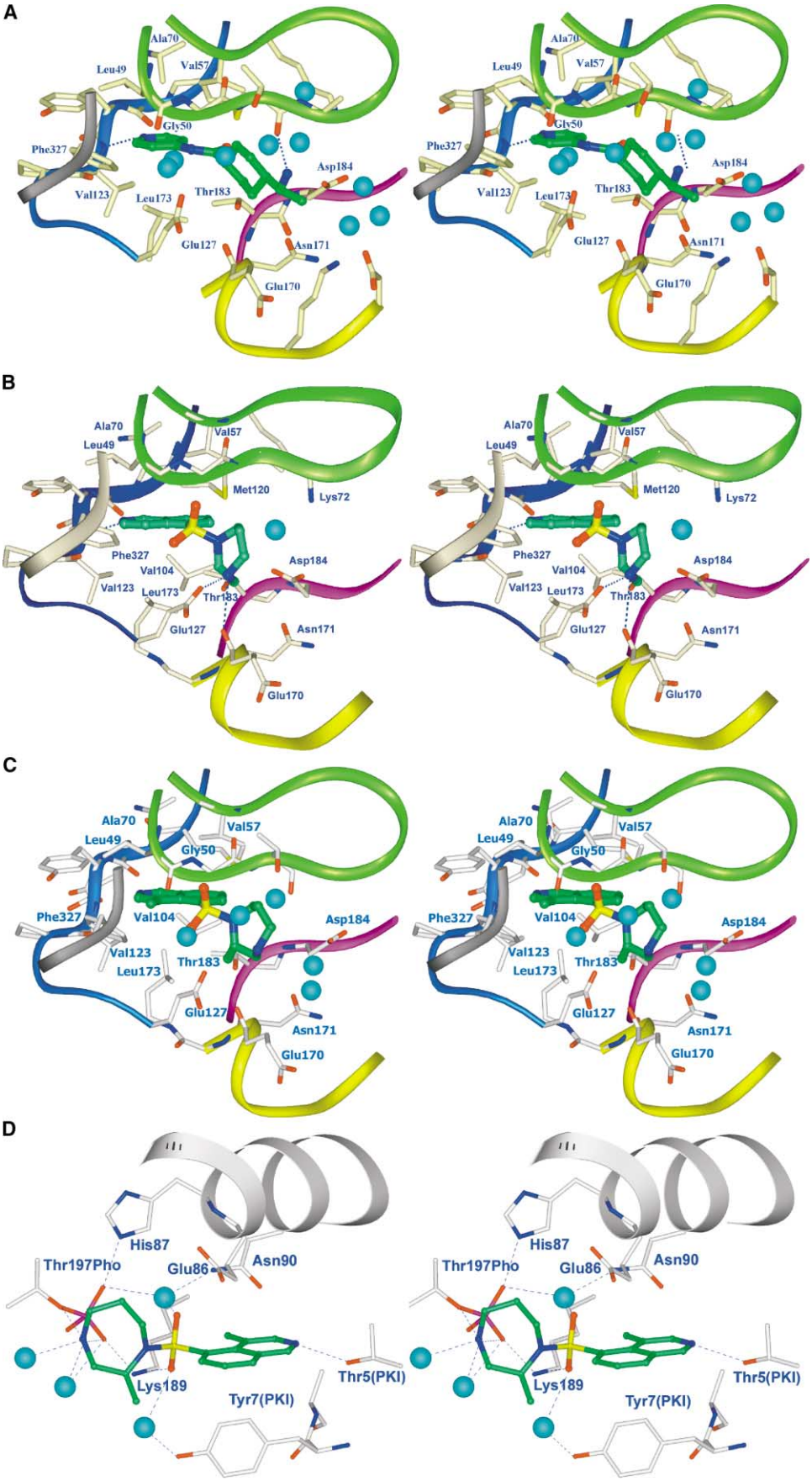

Figure 5. Inhibitor Binding Modes

Binding of Y-27632 (A) and HA-1077 (B) to PKA to the ATP binding site. H-1152P binds in two positions: (C) in the ATP binding site and (D) in a second binding site at the surface interacting with the activation loop and helix C in a crystal contact region.

Table 4. H Bonds between Inhibitor Atoms and PKA Enzyme Residues

H Bonds	Inhibitor Atom	PKA Residue and Atom	Distance (Å)	Interaction via
Y-27632 chair 1	N1	Val123(N)	2.9	main chain
	N17	Thr51(O)	2.8	side chain
Y-27632 chair 2	N1	Val123(N)	2.9	main chain
	N17	Glu171(OD1)	2.9	side chain
	N17	Asp184(OD1)	2.9	side chain
HA-1077	N15	Val123(N)	2.8	main chain
	N4	Glu170(O)	3.3	main chain
	N4	Glu127(OE2)	2.7	side chain
H-1152P	N16	Val123(N)	3.0	main chain

H bonds between inhibitor and PKA atoms are listed together with the distance (in Å) and information about main chain or side chain interaction.

homolog, and, in addition, further contacts to the homologs of the Val123 and/or Glu121 carbonyl atom(s). This interaction is conserved despite the wide chemical diversity of small molecule protein kinase inhibitors. Thus the interaction is critical for good inhibitors, or conversely stated, the kinase is apparently unable to compensate for the desolvation of the Val123NH equivalent group if a potential inhibitor lacks the appropriate hydrogen bond acceptor. Hydrogen bonds from other residues that bind to the adenosine group of ATP appear to be of less importance for protein kinase inhibitor binding. Two H bonds that are formed between the ribosyl hydroxyl groups of AMP-PNP and the Glu127 carboxyl and the Glu170 main chain carbonyl groups have counterparts in the PKA-1077 structure. The presumably doubly protonated secondary amine (N4) of HA-1077 forms hydrogen bonds both to the carboxyl group of Glu127 and to the backbone carbonyl of Glu170. In the case of H-1152P, these contacts are not formed, because contacts between Thr183 and Leu173 of the enzyme and homopiperazine methyl group (C10) of the inhibitor apparently shift the heptamer ring by ca. 1.5 Å in comparison to HA-1077. Consequently, the distances to E170(O) (4.2 Å) and E127 (OD1) (3.57 Å) are too large for tight H bonds. The overlay of the two structures in Figure 6 shows the colocalization of the isoquinoline atoms with respect to the surrounding residues, and the divergent positions of the homopiperazine rings. Although H-1152P makes only one hydrogen bond to the enzyme, the two extra methyl groups increase the number of van der Waals interactions (Table 3) and enlarge the buried surface area, which probably leads to the enhanced affinity of H-1152 in comparison to HA-1077.

The Second Binding Site of H-1152P

The second molecule of H-1152P in PKA-1152P is found in contact with the activation segment and helix C, the two structural elements critical for protein kinase inactivation (Engh and Bossemeyer, 2001), which suggests a potential for activity modulation. Because the residues in contact with this second inhibitor molecule are not conserved between PKA and Rho-kinase, the observed second H-1152P binding site likely appears to be unique for PKA. Further, this site is an important contact region for protein-protein interaction with the regulatory subunits of PKA (Orellana et al., 1993; Gibbs et al., 1992). Occupation of this site with a small molecule derivative could provide a means to abolish negative regulation of PKA by the R subunits. If this site could be explored more generally as a docking site for small molecules in drug design, other important interactions, for example cyclin binding to cyclin-dependent kinases, could be targeted as well.

Comparison of the Rho-Kinase and PKA Ligand Binding Sites

Although the three inhibitors bind and inhibit PKA, all of them bind Rho-kinase more tightly than PKA. Because of the high conservation of the protein kinase fold, especially for closely related kinases, one can assume that the side chains that are nearest to the inhibitor are the major determinants of selectivity. The sequence alignment of the kinase domains of Rho-kinase and PKA (Figure 2) show either conservation (blue coloring) or conservative exchanges (beige coloring) over large parts of the kinase domain. Rho-kinase has several exchanges relative to PKA, but only four of them make side chain interactions with the inhibitors: Thr183Ala, Leu49Ile, Val123Met, and Glu127Asp. These exchanges very likely are responsible for the effects of the extra methyl groups of H-1152P compared to HA-1077 on specificity toward Rho-kinase. The two methyl groups lead to a 200-fold higher affinity for Rho-kinase (Table 2), but only a 2- to 5-fold higher affinity for PKA, or in other words, cause a 40- to 100-fold increase in selectivity.

The residues nearest to the H-1152P methyl groups are Leu49, Leu173, Thr183, and Phe 327, thus involving directly two of these four PKA to Rho-kinase exchanges, and one residue (Phe 327) specific for most AGC kinases. The Thr183Ala substitution would provide more room for the C10 methyl group and possibly allow more rotamer conformations of Leu173. The interactions of C10 with Thr183 and Leu173 in PKA appear to force the H-1152P homopiperazine away from its position in the PKA-1077 structure (Figure 6), presumably at some energy cost. The exchange of Thr183Ala in Rho-kinase would, however, allow the homopiperazine to retain its preferred binding orientation. Consequently, H-1152P might be able to form hydrogen bonds to both the Glu170 homolog and to the aspartyl residue occupying the Glu127 homologous position in Rho-kinase. Although the side chain of the aspartyl is shorter by one methylene group, this should not affect its ability to hydrogen bond a homopiperazine nitrogen in a position similar to that of HA-1077 in PKA.

The effect of the Leu49Ile exchange is more difficult to evaluate because of the number of possible rotamer

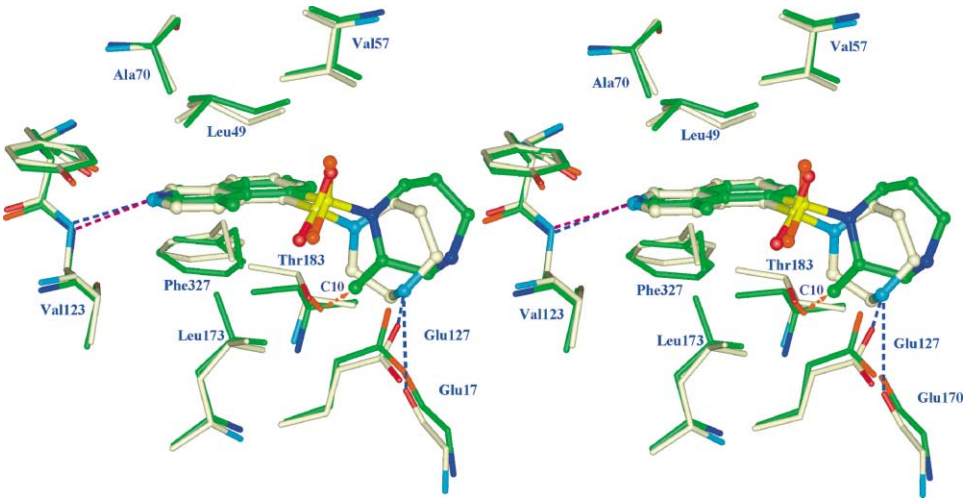

Figure 6. Comparison of HA-1077 and H-1152P

Overlay of HA-1077 and H-1152P demonstrates the colocalization of the isoquinoline atoms with respect to the surrounding residues. Both inhibitor molecules form an H bond to the backbone amide of Val123 in the hinge region. The position of the homopiperazine rings, however, diverge by ca. 1.5 Å. Consequently, H bonds between the homopiperazine nitrogen and Glu127 and Glu170 are formed only in the PKA-1077 complex. The contact between C10 and Thr183, which prevents as a steric clash a HA-1077-like positioning of the H-1152P homopiperazine ring, is shown as a red double arrow.

conformations of the isoleucine residue. Most rotamers of an isoleucine modeled into the Leu49 position increase the number of interactions with the inhibitor or cause steric clashes with the inhibitor isoquinoline sulfonamide moiety. Because of the branching of the isoleucine side chain at the Cβ, in contrast to a leucine residue, the inhibitor binding pocket is narrowed in the expected binding region of the isoquinoline methyl and sulfonamide groups, also close to the Phe327 homolog; this appears to favor H-1152P binding. It is likely that the isoquinoline methyl group of H-1152P then additionally contributes to a productive interaction by a mutual increase in the number of van der Waals interactions with the isoleucine side chain.

How or even whether the Val123Met exchange might affect binding selectivity is unclear. A relatively large number of van der Waals contacts (Table 3) are formed to all three inhibitors. A methionine residue is found at this position in several kinases with known structures, including Erk, p38, Src, and Abl. In all these cases, the methionine side chain is oriented away from the adenosine subsite, providing little contact beyond the Cγ atom. By analogy, this methionine side chain therefore is not likely to be a major factor in H-1152P specificity for Rho-kinase. In addition, a large number of van der Waals contacts are found with the residue Phe327, which is conserved in most members of the AGC group of protein kinases. Phe327 makes attractive additional interactions with the isoquinoline extra methyl group of H-1152P in PKA, compared to HA-1077.

Taken together, the higher affinities of HA-1077 and H-1152P for Rho-kinase—and the especially strong binding of the H-1152P derivative to Rho-kinase—can be explained largely by *three* factors: the Thr183Ala exchange and the concomitant relaxation of the steric clash between the inhibitor C10 methyl group and Thr183 and Leu173 (Figure 6). This in turn allows the inhibitor to bind with the optimal geometry and hydrogen bonding pattern as observed for HA-1077 in PKA. Further, the exchange Leu49Ile presumably optimizes the van der Waals interactions—i.e., inhibitor fit—because of the position of the branch in the side chain. Whether additional effects arise from the Val123Met exchange remains to be seen. Last but not least, the AGC-kinase typical Phe327 residue makes attractive contacts with all inhibitors, but especially with the C22 extra methyl group of H-1152P.

The higher affinity of Y-27632 for Rho-kinase is more difficult to rationalize based on sequence considerations. One determinant is probably the Leu49Ile exchange. The shorter branched methyl group is likely to provide additional van der Waals interactions with three different parts of the inhibitor molecule, thereby increasing the overall binding surface area and improving the quality of the fit. The absence of steric clashes in the region of Thr183 (and Glu127), however, obscures analysis of possible contributions of the corresponding exchanges at these positions to the higher affinity of Y-27632 in Rho-kinase. Regarding the Val123Met exchange, the likelihood that it is oriented away from the inhibitor as discussed above leads to the conclusion that Rho-specific interactions with the Met side chain are possible but unlikely. A similar compound, Y-30141, which differs from Y-27632 by a pyrrolopyridine ring replacing the pyridine ring, has a similar inhibitory profile, but a 10-fold higher affinity for Rho-kinases (Ishizaki et al., 2000). Its selectivity, i.e., the ratios of the IC50 for Rho-kinase to that for other kinases, however, is about 10-fold lower. In the binding pocket, the extra pyrrolidine group is likely to make one additional hinge region contact with its proton donor in the five ring, either to the carbonyl of Glu121 (PKA numbering) or, if rotated 80°, to the carbonyl of Val123. The higher affinity can also be explained by the larger surface of the planar double

Table 5. Conservation of Residues in the Binding Pocket that Differ between PKA and Rho-Kinase

Residue in PKA	PKA	No.*	%	Rho kinase	No.*	%	Contact
49	Leu	241	49.1	Ile	186	37.9	**side chain**/backbone
51	Thr	18	3.7	Arg	71	14.5	backbone only
123	Val	76	15.5	Met	123	25.1	**side chain**/backbone
127	Glu	76	15.5	Asp	158	32.2	**side chain**
170	Glu	140	28.5	Asp	59	12.0	backbone only
183	Thr	76	15.5	Ala	142	28.9	**side chain**

Shown are residues in contact with the inhibitors that differ between PKA and Rho-kinase according to the alignment from www.kinase.com (Manning et al., 2002). The total number of kinases in the alignment is 491. The number (No.*) as well as percentage (%) of kinases with the same corresponding residue (numbering according to PKA) to PKA and Rho-kinase, respectively, were calculated. Contacts to the inhibitor via main chain or side chain are indicated. Residues that have side chain contacts with the ATP-site ligands are in bold.

ring compared to the single ring of Y-27632. These additional interactions can be assumed to increase the binding potency. The drop in selectivity can be explained if one assumes that the interactions which determine the selectivity for these Y-class inhibitors remain the same for both inhibitors and thus are less relevant in the case of the better binding Y-30141.

Selectivity of the Inhibitors for Rho-Kinase Relative to Other Kinases

We have argued above that many of the interactions with residues which differ between Rho-kinase and PKA explain why HA-1077, H-1152P, and Y-27632 bind more tightly to Rho-kinase than to PKA. The amino acid residues in question are, however, common in the kinase family. From the available kinetic data, at least HA-1077 and Y-27632 show selectivity for only a few kinases (less data is available for H-1152P). The question arises whether selectivity arises from a unique combination of specific amino acid residues or simply from the sum of a small number of individual interactions that can be considered independently of one another.

Using a sequence alignment of 491 human kinases (see e.g., www.kinase.com; Manning et al., 2002), we built a database to calculate the frequency of certain amino acid residues and of their combinations. Table 5 shows the degree of conservation for the residues that are different between PKA and Rho-kinase. Either isoleucine and leucine is found at the Leu49 position in most kinases, with leucine more frequent than isoleucine. Also, an alanine in the Thr183 position (28.9%) is common (and more common than threonine with 15.5%). Relatively high frequencies are found also for Rho-kinase side chains of methionine in the Val123 position (25.1%) and aspartic acid at the Glu127 position (32.2%). While these residues are common when considered individually, the combination of all four is nearly unique. Only 6 out of 491 kinases possess the same combination, 3 from the subgroup of cell cycle related kinases (CRK7, CCRK, and CHED), and 3 tyrosine kinases, MUSK, MET and RON.

If we consider additionally the AGC characteristic residue Phe327, the combination of inhibitor binding side chains seen in Rho-kinase becomes truly unique. Phe327, located on a C-terminal strand that stretches across the catalytic cleft, interacts with its aromatic side chain with the adenosine moiety of ATP, as well as with all kinase inhibitors cocrystallized with PKA so far. The three inhibitors in this study make four (Y-27632), six (HA-1077), or eight (H-1152P) van der Waals contacts to Phe327. Sequence alignments of PKA versus ROCK-I or ROCK-II indicate that Rho-kinase also has a phenylalanine residue in a position homologous to Phe327 (Figure 2). The crystal structure of AGC kinase PKB shows residue Phe439 in a position identical to Phe327 in PKA (Yang et al., 2002). More distantly related kinases, however, do not have a corresponding C-terminal strand with a recognizably equivalent aromatic side chain (although other strands, domains, or subunits may contribute a similar chain). Thus, the combination of all five residues, Ile (Leu49), Ala (Thr183), Asp (Glu127), Met (Val123), and Phe (Phe327), is an exclusive feature of Rho-kinase. It should be noted that these residues are also among the ones with the largest numbers of contacts to the inhibitors, especially to H-1152P (Table 3). And, while the individual residues exchanges may be relatively conserved, in combination they generate a uniquely shaped inhibitor binding pocket with unique electronic properties, rationalizing the selectivity of Rho-kinase for certain protein kinase inhibitors, such as HA-1077, H-1152P, and Y-27632.

Conclusions

The one common feature of all protein kinases is ATP binding at a highly conserved ATP binding site with highly conserved binding interactions. The highest degree of conservation is seen with the catalytic residues that are absolutely conserved across the entire protein kinase family. The tertiary structure that forms the ATP binding site is apparently highly conserved in the active state of the protein, but this conclusion depends upon extrapolation from the still relatively few active structures that have been solved. The primary sequences are mostly highly conserved at the residues that form the triphosphoryl binding site, presumably because this represents the catalytic site. Conserved features of the adenosine binding site are restricted to the backbone contacts of the hinge region and to a generally hydrophobic or aromatic environment surrounding adenine; residues at positions homologous to Val57 and Ala70 in PKA are additionally conserved as small hydrophobic residues. Otherwise, there is considerable variability in sequence and, when considering inactive forms, in structure among protein kinases. Physiological

roles for this variability are generally recognized only for those cases where specific events such as phosphorylation are seen to modulate activity. Most protein kinases bind ATP with low micromolar binding constants, consistent with the need for exchange of ATP, ADP, and unbound states. Thus, sequence and structural variability at the ATP binding pocket has few known physiological roles regarding ATP binding, but is crucial for the selectivity of nonphysiological, high affinity ATP-site ligands, such as low molecular weight protein kinase inhibitors.

Crystallographic studies of enzyme-inhibitor complex structures provide information directly relevant to the drug design tasks of optimizing potency and selectivity. For protein kinases, these tasks are complicated by several factors. First, the substrate binding sites are relatively flexible, so that individual structures do not fully characterize an enzyme. Secondly, as discussed above, the natural substrates generally bind weakly, so that tight binding inhibitors are not obviously derivable from substrates. Third, the similarity of the ATP binding sites of active protein kinases means that inhibitors are likely to bind many of the ca. 600 kinases other than the target kinase.

The development of potent and selective kinase inhibitors and their success as therapeutics has demonstrated that problems anticipated with protein kinases as targets can be overcome. The process of optimization of such inhibitors can be improved. Of the inhibitors described here, only H-1152P was specifically designed to target Rho-kinase. The crystal structures, however, show how they bind and identify the probable determinants of Rho-kinase selectivity. This information focuses strategies for chemical synthesis and should improve the overall efficiency in achieving desired inhibition profiles. Cocrystal structures of Rho-kinase with inhibitors are needed to verify and possibly refine the model. Verification of the model would also verify the approach of using PKA as a surrogate for Rho-kinase crystallization, which might remain a preferable approach if Rho-kinase crystallization proves difficult, or if only inactive conformations of Rho-kinase will be crystallizable.

Experimental Procedures

Protein Expression and Purification

Recombinant bovine Cα catalytic subunit of cAMP-dependent protein kinase (which differs from the human protein at two positions: Asn32Ser and Met63Lys) was soluble expressed in *E. coli* BL21(DE3) cells and then purified via affinity chromatography and ion exchange chromatography as previously described (Engh et al., 1996). Threefold phosphorylated protein was used for crystallization of Y-27632 and H-1152P, whereas 4-fold phosphorylated protein successfully formed cocrystals with HA-1077.

Crystallization

Y-27632 and HA-1077 were purchased from Calbiochem. Y-27632, HA-1077, and H-1152P were cocrystallized with PKA and PKI(5-24) at 75 mM LiCl, 25 mM MesBisTris (pH 6.4). Hanging drop vapor diffusion against 15% methanol as precipitant was used to obtain ca. 100 × 100 × 500 μm crystals.

Biacore Sensor Chip Preparation

Proteins used for Biacore analysis were dialyzed two times with the 400-fold volume of 50 mM MOPS (pH 6.8), 10 mM $MgCl_2$, and 50 mM KCl (Gassel et al., 2003). Coupling of PKA to a CM5 Biasensor chip via amine group linkage was achieved using standard coupling procedures (Löfås and Johnsson, 1990). Briefly, CM5 sensor chips were activated by injecting 35 μl of a 1:1 mixture of N-ethyl-N′-[dimethylamino]carbodiimide/N-hydroxysuccinimide at 5 μl/min. After diluting the proteins in 10 mM sodium acetate (pH 5.5), PKA (with HSA as a control) was coupled to the CM5 sensor chip by injecting a 50 μM solution of the protein selected with a flow rate of 5 μl/min until 11,000 RU was reached.

Generation of Kinetic Binding Data

Kinetic studies with a range of analyte concentrations were determined at a flow rate of 10 μl/min by allowing 300 s for association and 900 s for dissociation. Analytes were diluted in MilliQ water or running buffer (50 mM MOPS [pH 7.4], 50 mM KCl, and 10 mM $MgCl_2$). Kinetic data were analyzed with BIAevaluation 3.0 software. For each binding curve, the response obtained using the HSA cell as control was subtracted. Due to the small signals (up to 40 RU), the steady-state affinity model was used to determine the K_i of the different small molecular weight compounds. Goodness of fit (measured as χ^2) was less than 5 for binding of the low molecular weight compounds. All binding experiments were repeated two times, and biosensor chips coupled at different times yielded surfaces with identical binding affinities. The binding affinities of H-1152P, HA-1077, and Y-27632 to PKA were similar to the K_i values reported in different studies (Sasaki et al., 2002; Uehata et al., 1997) and citations therein, using enzymatic assays.

Data Collection and Structure Determination

Diffraction data were measured at 4°C in a sealed capillary on an image plate detector (Mar research) or Bruker X1000 area detector using a copper target Rigaku Rotaflex X-ray generator and graphite crystal K_α monochromator. In each case one crystal was sufficient to obtain a complete data set. The data were processed with the programs MOSFLM and SCALA or ASTRO and SAINT. All crystals have an orthorhombic symmetry ($P2_12_12_1$) with similar cell constants (Table 1). The structures were determined by molecular replacement using the CCP4 program package (www.ccp4.ac.uk/main/html). As a starting model we chose a PKA structure in a closed conformation (our unpublished data). Refmac 5.1.24 was used for refinement, while MOLOC was used (www.moloc.ch) for graphical evaluation and model building.

Surface Calculations

Buried surfaces were calculated with the program Insight II (Accelrys). The total surface of the isolated inhibitor and the accessible surface of the inhibitor in the complex were calculated. The difference is the buried surface.

Sequence Alignment and Homology Model Building

Sequences were aligned using the ClustalW server from http://www.ebi.ac.uk/clustalw/. The homology model was calculated by the SWISS-MODEL Protein Modelling Server (http://www.expasy.ch/swissmod/SWISS-MODEL.html).

Acknowledgments

We thank Norbert König for expert technical assistance and Wolf Lehmann for verifying enzyme purity by mass spectrometry.

Received: May 30, 2003
Revised: August 14, 2003
Accepted: August 14, 2003
Published: December 2, 2003

References

Akamine, P., Madhusudan, Wu, J., Xuong, N.H., Eyck, L.F.T., and Taylor, S.S. (2003). Dynamic features of cAMP-dependent protein kinase revealed by apoenzyme crystal structure. J. Mol. Biol. *327*, 159–171.

Amano, M., Ito, M., Kimura, K., Fukata, Y., Chihara, K., Nakano, T., Matsuura, Y., and Kaibuchi, K. (1996). Phosphorylation and activa-

tion of myosin by Rho-associated kinase (Rho-kinase). J. Biol. Chem. *271*, 20246–20249.

Amano, M., Fukata, Y., and Kaibuchi, K. (2000). Regulation and functions of Rho-associated kinase. Exp. Cell Res. *261*, 44–51.

Battistutta, R., Sarno, S., De Moliner, E., Papinutto, E., Zanotti, G., and Pinna, L.A. (2000). The replacement of ATP by the competitive inhibitor emodin induces conformational modifications in the catalytic site of protein kinase CK2. J. Biol. Chem. *275*, 29618–29622.

Bossemeyer, D., Engh, R.A., Kinzel, V., Ponstingl, H., and Huber, R. (1993). Phosphotransferase and substrate binding mechanism of the cAMP-dependent protein kinase catalytic subunit from porcine heart as deduced from the 2.0 A structure of the complex with Mn2+ adenylyl imidodiphosphate and inhibitor peptide PKI(5–24). EMBO J. *12*, 849–859.

Davies, S.P., Reddy, H., Caivano, M., and Cohen, P. (2000). Specificity and mechanism of action of some commonly used protein kinase inhibitors. Biochem. J. *351*, 95–105.

Engh, R.A., and Bossemeyer, D. (2001). The protein kinase activity modulation sites: mechanisms for cellular regulation—targets for therapeutic intervention. Adv. Enzyme Regul. *41*, 121–149.

Engh, R.A., and Bossemeyer, D. (2002). Structural aspects of protein kinase control: role of conformational flexibility. Pharmacol. Ther. *93*, 99–111.

Engh, R.A., Girod, A., Kinzel, V., Huber, R., and Bossemeyer, D. (1996). Crystal structures of catalytic subunit of cAMP-dependent protein kinase in complex with isoquinolinesulfonyl protein kinase inhibitors H7, H8, and H89. Structural implications for selectivity. J. Biol. Chem. *271*, 26157–26164.

Fukata, Y., Amano, M., and Kaibuchi, K. (2001). Rho-Rho-kinase pathway in smooth muscle contraction and cytoskeletal reorganization of non-muscle cells. Trends Pharmacol. Sci. *22*, 32–39.

Gassel, M., Breitenlechner, C.B., Ruger, P., Jucknischke, U., Schneider, T., Huber, R., Bossemeyer, D., and Engh, R.A. (2003). Mutants of protein kinase a that mimic the ATP-binding site of protein kinase B (AKT). J. Mol. Biol. *329*, 1021–1034.

Gibbs, C.S., Knighton, D.R., Sowadski, J.M., Taylor, S.S., and Zoller, M.J. (1992). Systematic mutational analysis of cAMP-dependent protein kinase identifies unregulated catalytic subunits and defines regions important for the recognition of the regulatory subunit. J. Biol. Chem. *267*, 4806–4814.

Hidaka, H., Inagaki, M., Kawamoto, S., and Sasaki, Y. (1984). Isoquinolinesulfonamides, novel and potent inhibitors of cyclic nucleotide dependent protein kinase and protein kinase C. Biochemistry *23*, 5036–5041.

Ikenoya, M., Hidaka, H., Hosoya, T., Suzuki, M., Yamamoto, N., and Sasaki, Y. (2002). Inhibition of Rho-kinase-induced myristoylated alanine-rich C kinase substrate (MARCKS) phosphorylation in human neuronal cells by H-1152, a novel and specific Rho-kinase inhibitor. J. Neurochem. *81*, 9–16.

Ishizaki, T., Uehata, M., Tamechika, I., Keel, J., Nonomura, K., Maekawa, M., and Narumiya, S. (2000). Pharmacological properties of Y-27632, a specific inhibitor of Rho-associated kinases. Mol. Pharmacol. *57*, 976–983.

Itoh, K., Yoshioka, K., Akedo, H., Uehata, M., Ishizaki, T., and Narumiya, S. (1999). An essential part for Rho-associated kinase in the transcellular invasion of tumor cells. Nat. Med. *5*, 221–225.

Johnson, D.A., Akamine, P., Radzio-Andzelm, E., Madhusudan, and Taylor, S.S. (2001). Dynamics of cAMP-dependent protein kinase. Chem. Reviews *101*, 2243–2270.

Löfås, S., and Johnsson, B. (1990). A novel hydrogel matrix on gold surfaces in surface plasmon resonance sensors for fast and efficient covalent immobilization of ligands. J. Chem. Soc. Chem. Commun. *21*, 1526–1528.

Manning, G., Whyte, D.B., Martinez, R., Hunter, T., and Sudarsanam, S. (2002). The protein kinase complement of the human genome. Science *298*, 1912–1934.

Matsui, T., Amano, M., Yamamoto, T., Chihara, K., Nakafuku, M., Ito, M., Nakano, T., Okawa, K., Iwamatsu, A., and Kaibuchi, K. (1996). Rho-associated kinase, a novel serine threonine kinase, as a putative target for the small GTP binding protein Rho. EMBO J. *15*, 2208–2216.

Narayana, N., Diller, T.C., Koide, K., Bunnage, M.E., Nicolaou, K.C., Brunton, L.L., Xuong, N.H., Ten Eyck, L.F., and Taylor, S.S. (1999). Crystal structure of the potent natural product inhibitor balanol in complex with the catalytic subunit of cAMP-dependent protein kinase. Biochemistry *38*, 2367–2376.

Ono-Saito, N., Niki, I., and Hidaka, H. (1999). H-series protein kinase inhibitors and potential clinical applications. Pharmacol. Ther. *82*, 123–131.

Orellana, S.A., Amieux, P.S., Zhao, X., and McKnight, G.S. (1993). Mutations in the catalytic subunit of the cAMP-dependent protein kinase interfere with holoenzyme formation without disrupting inhibition by protein kinase inhibitor. J. Biol. Chem. *268*, 6843–6846.

Prade, L., Engh, R.A., Girod, A., Kinzel, V., Huber, R., and Bossemeyer, D. (1997). Staurosporine-induced conformational changes of cAMP-dependent protein kinase catalytic subunit explain inhibitory potential. Structure *5*, 1627–1637.

Sasaki, Y., Suzuki, M., and Hidaka, H. (2002). The novel and specific Rho-kinase inhibitor (S)-(+)-2-methyl-1-[(4-methyl-5-isoquinoline) sulfonyl]-homopiperazine as a probing molecule for Rho-kinase-involved pathway. Pharmacol. Ther. *93*, 225–232.

Shimokawa, H., Iinuma, H., Kishida, H., Nakashima, M., and Kato, K. (2001). Antianginal effect of fasudil, a Rho-kinase inhibitor, in patients with stable effort angina: a multicenter study. Circulation *104*, 2843.

Sinnett-Smith, J., Lunn, J.A., Leopoldt, D., and Rozengurt, E. (2001). Y-27632, an inhibitor of Rho-associated kinases, prevents tyrosine phosphorylation of focal adhesion kinase and paxillin induced by bombesin: dissociation from tyrosine phosphorylation of p130(CAS). Exp. Cell Res. *266*, 292–302.

Tanaka, H., Ohshima, N., Takagi, M., Komeima, K., and Hidaka, H. (1998). Novel vascular relaxant, Hmn-1152: its molecular mechanism of action. Naunyn-Schmied. Arch. Pharmacol. *358*, P3740.

Trauger, J.W., Lin, F.F., Turner, M.S., Stephens, J., and LoGrasso, P.V. (2002). Kinetic mechanism for human Rho-Kinase II (ROCK-II). Biochemistry *41*, 8948–8953.

Uehata, M., Ishizaki, T., Satoh, H., Ono, T., Kawahara, T., Morishita, T., Tamakawa, H., Yamagami, K., Inui, J., Maekawa, M., and Narumiya, S. (1997). Calcium sensitization of smooth muscle mediated by a Rho-associated protein kinase in hypertension. Nature *389*, 990–994.

Yang, J., Cron, P., Good, V.M., Thompson, V., Hemmings, B.A., and Barford, D. (2002). Crystal structure of an activated Akt/protein kinase B ternary complex with GSK3-peptide and AMP-PNP. Nat. Struct. Biol. *9*, 940–944.

Accession Numbers

Atomic coordinates have been deposited in the Protein Data Bank with accession numbers 1Q8T, 1Q8U, and 1Q8W.